كلية الهندسة بشبرا
FACULTY OF ENGINEERING AT SHOUBRA
ERJ
PRINT ISSN 3009-6049
ONLINE ISSN 3009-6022

ENGINEERING RESEARCH JOURNAL (ERJ)
Volume (53) Issue (1)
January 2024, pp:130-141
https://erjsh.journals.ekb.eg

Investigating the Influence of Tool Selection on Surface Quality in Burnished AISI 1035 Steel

Mahmoud Elsamanty [1,2], Waleed F. Youssef [*], M. Abdelsalam [3], A. A. Ibrahim [1]

[1] *Department of Mechanical Engineering Department, Faculty of Engineering at Shoubra, Benha University,*
[2] *Department of Mechatronics and Robotics, School of Innovative Engineering Design, Egypt-Japan University of Science and Technology (E-JUST), Alexandria, Egypt.*
[3] *Department of Design and production engineering - faculty of Engineering - Ain Shams University, Cairo, Egypt*
[*] *Corresponding Author.*
E-mail: *mahmoud.alsamanty@feng.bu.edu.eg, mahmoud.elsamanty@ejust.edu.eg, w.farag25751@feng.bu.edu.eg, Mohamed.Abdelsalam@eng.asu.edu.eg, abdelkader.ibrahim@feng.bu.edu.eg*

Abstract: The metal burnishing process is a vital and modern technique for achieving high-quality surface finishes. This research uses the Taguchi and RSM (Response Surface Methodology) methods to optimize the ball burnishing process parameters. Three different tools were specifically designed and utilized in this study, and a Taguchi L16 matrix was employed for the experimental design. The results of surface roughness parameters and surface out-of-roundness were conducted. The resulting data was subjected to square regression analysis. The findings of this research demonstrate that both the tool type selected as well as the burnishing parameters significantly influence the surface roughness and out-of-roundness values. The analysis revealed intricate relationships between these factors, providing valuable insights for process optimization. Specifically, the research identified optimal parameter combinations for each tool type, leading to improved surface quality. The rigid tool exhibited minimum surface roughness at a rotational speed of 450 RPM, a feed rate of 0.09 mm/rev, and a penetration depth of 0.35 mm. While the spring tool achieved minimum surface roughness at a rotational speed of 500 RPM, a feed rate of 0.09 mm/rev, and a penetration depth of 0.35 mm. For out-of-roundness, the rigid tool exhibited minimum out-of-roundness at a rotational speed of 600 RPM, a feed rate of 0.12 mm/rev, and a penetration depth of 0.35 mm. While the spring tool achieved minimum out-of-roundness at a rotational speed of 475 RPM, a feed rate of 0.09 mm/rev, and a penetration depth of 0.20 mm. Additionally, the pneumatic tool yielded minimum surface roughness at a rotational speed of 600 RPM, a feed rate of 0.11 mm/rev, and a depth of penetration of 0.20 mm, with minimum out-of-roundness achieved at a rotational speed of 300 RPM, a feed rate of 0.10 mm/rev, and a depth of penetration of 0.20 mm.

Keywords: Surface Roughness, Out-of-Roundness, Rigid Tool, Spring-Assisted Tool, Pneumatic Tool.

1. INTRODUCTION

The performance of mechanical components is significantly influenced by surface topography characteristics including, but not limited to, roughness, contour, and geometrical form accuracy [1]. Precise surface topography becomes especially critical for applications that demand fluid sealing, low friction, or tight clearances. The burnishing process, a revolutionary surface finishing technique that does not generate chips, utilizes mechanical surface treatment to improve the properties of previously machined surfaces [2,3]. It compacts the surface asperities using pressures exceeding the material's yield strength. This leads to a restructured workpiece material without material removal, refining the microstructure and providing a superfine surface finish.

The fundamental methodology behind burnishing involves rolling a hard tool, such as a ball or a roller, against the workpiece surface while applying forced contact through a loading system [4,5]. Intense plastic deformation occurs locally at the workpiece surface when the yield point is exceeded. This 'cold working' process compresses, and work hardens the material, forming a thin, smooth, and dense layer of reconsidered grains [6]. As a result, the treated surface exhibits reduced roughness, and increased resistance to corrosion and wear. Precise control of burnishing parameters can optimize these surface enhancements for demanding functional requirements.

Previous research has demonstrated the effectiveness of the burnishing technique in enhancing significant surface characteristics through mechanical surface treatment [2,4]. However, there is less exploration of burnishing's influence over other critical surface geometry attributes that define functional performance. Further study is needed to characterize burnishing's capabilities to control deviations from ideal geometrical form, such as out-of-roundness [2,4]. As manufacturing tolerances progressively tighten to meet precision requirements in applications involving fluid sealing, coefficient of friction control, and miniature clearances, understanding how surface shaping methods like burnishing sculpt very near-surface geometry becomes imperative [7,8].

Previous research has also identified opportunities to optimize process parameters to reduce energy consumption during surface treatment while enhancing surface quality [9]. For instance, it has been observed that surface roughness decreases with increasing burnishing speed, reaching a minimum value before rising again at higher speeds [10]. This trend is attributed to the increasing deformation of irregular micro-scale ridges and valleys with faster relative tool-work motions [11]. However, when burnishing velocity surpasses optimal, insufficient straining occurs to refine irregularities before the tool passes [12].

Increasing the burnishing depth affects the resulting surface roughness, with deeper burnishing depths producing greater plastic deformation within the workpiece material [12,13]. However, most studies have focused on characterizing burnishing's influence on surface roughness alone.

Increasing the burnishing depth initially reduces out-of-roundness until it reaches a specific value, beyond which further increase cause the surface layers to overharden and perhaps flake, which increases out-of-roundness [14].

Out-of-roundness, an important burnishing-induced surface attribute, requires further characterization to understand its influencing factors. Previous work found that as burnishing speed increased, out-of-roundness measurements improved due to a concurrent rise in temperature at the ball-workpiece interface, which temporarily softened the deformed material [15]. However, reducing process time by increasing the burnishing feed rate inflicts an ineffective burnishing emphasis on localized regions, thus raising out-of-roundness errors.

While previous experimental observations provide preliminary insight, systematic characterization across controlled burnishing settings is still necessary. There is a lack of understanding about burnishing's capability to control deviations from a desired geometric form, such as out-of-roundness. As manufacturing tolerances continue to tighten in line with the precision demands of modern designs, it is increasingly important to quantify how surface finishing techniques like burnishing sculpt very near-surface geometry. Therefore, informed by an extensive review of existing literature and the recognized gaps in the comprehension of the effects of burnishing parameters on surface roughness and out-of-roundness, this research aims to quantify burnishing parameter influence on AISI 1035 steel specimens' surface texture and form accuracy. By defining process windows that target the simultaneous optimization of functional surface metrics like roughness alongside geometrical precision goals such as minimized out-of-roundness, this study will contribute to the broader field of mechanical component manufacturing.

For the research point three different tools, with different ball pressing mechanisms, were delivered, designed, and manufactured under specific conditions. The first tool type is a rigid burnishing tool that uses a rigid floating pressure mounted on the tool shank to press the ball against the workpiece. The burnishing load transferred by this tool is high compared to the other tools, but the ball life is shorter than other tools due to high friction between the tool and floating pressure device. The second tool is a tool uses a heavy loaded spring with a high stiffness value mounted on the tool shank to press the ball against the workpiece, the load transferred by this tool is smaller than the rigid tool, but the ball life is longer due to the low friction transferred to the burnishing ball surface. The third tool uses the power produced by an air compressor to transfer the burnishing force to the burnishing ball, a special mechanism is designed to press the ball against the workpiece using air pressure, the presence of air compressor is essential to the tool functionality leading to more expensive operation costs than the other tools used in this investigation.

2. EXPERIMENTAL INVESTIGATION

2.1 Workpieces

The workpiece material used in this research is St. 50, also known as AISI 1035 or C35 steel, a commonly used material in various industrial applications. St. 50, possesses specific properties that make it suitable for the intended

research purpose. It falls within the medium carbon steel category, with a carbon content of 0.35 percent by weight. Table 1 provides a comprehensive breakdown of the chemical composition of steel 50, highlighting the precise amounts of various elements present [16].

For more understanding, mean values of St. 50 mechanical properties are presented in Table 2 [16]. These include e.g., density, tensile strength, yield strength, modulus of elasticity, bulck modulus, shear modulus, and thermal conductivity. These properties provide crucial information about the material's strength, toughness, and ability to withstand different loading conditions. To evaluate the performance of the workpiece, a tension test was conducted on a rate of loading 0.1 mm/min according to ASTM E8/E8M standard on a standard tension test specimen, as illustrated in Figure 1 [17]. This test involves subjecting the specimen to gradually increasing tensile forces until failure occurs. The results of this tension test are depicted in Figure 2, showcasing the stress-strain relationship, and providing insights into the material's deformation behavior, ultimate strength, and fracture characteristics.

TABLE 1. Chemical composition of St. 50 (AISI 1035/C35) [16].

Grade	Chemical Composition %				
	Fe%	C%	Mn%	S%	P%
C35	98.80	0.35	0.70	0.005	0.004

TABLE 2. Comprehensive analysis of the mechanical properties of St. 50 (AISI 1035/C35) [16].

Grade	Density (g/cm^3)	Tensile Strength (MPa)	Yield Strength (MPa)	Modulus of Elasticity (GPa)	Bulck Modulus (GPa)	Shear Modulus (GPa)	Thermal Conductivity (W/mK)
C35	7.85	585	370	200	140	80	51.9

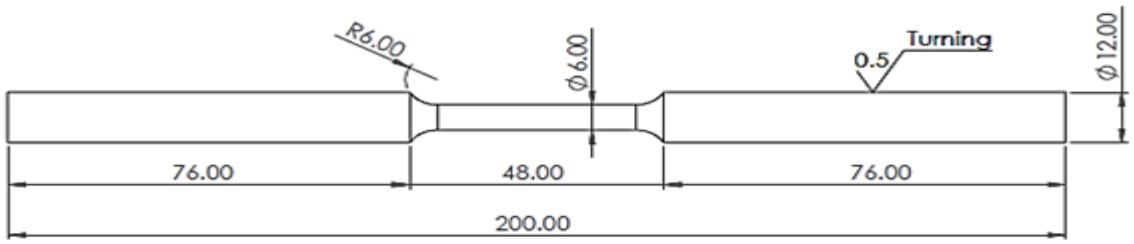

Fig 1. Tension test specimen according to ASTM E8/E8M standard [17].

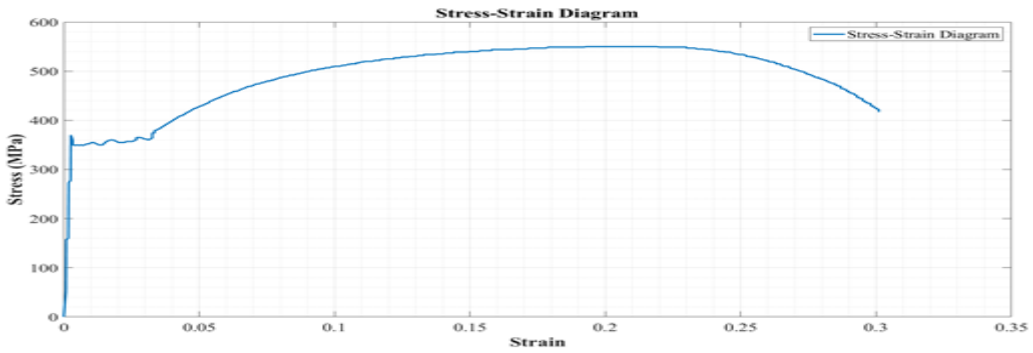

Fig 2. Stress-Strain curve of C35 steel from tensile test at 0.1 mm/min.

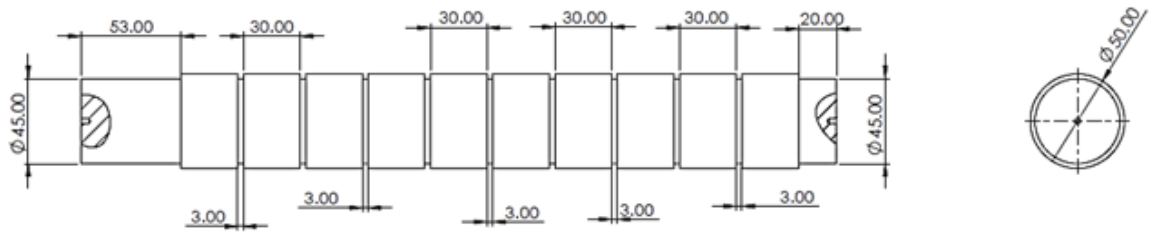

Fig 3. design of burnishing workpiece: a detailed representation of the workpiece configuration and features.

The workpieces were manufactured using a center lathe, a common machining tool for creating cylindrical components. In the production process, specific cutting settings were employed to shape the workpiece according to the desired specifications. These settings included a rotational speed of 600 RPM, a cutting feed of 0.1 mm/revolution, and a cutting depth of 0.1 mm. These parameters are crucial in achieving the desired surface finish, dimensional accuracy, and chip formation during machining. The workpiece was designed to have a diameter of 50 mm and a length of 400 mm with ten test portions of 30 mm long each, as outlined in Figure 3. The dimensions are important considerations for ensuring the workpiece's compatibility with other components or systems it will be integrated with. The configuration depicted in Figure 3 provides a data representation of the workpiece's overall shape, including any specific features, such as holes, threads, or grooves, that may be present.

2.2 Tools

In this work three types of burnishing tools are used: a delivered rigid tool, a custom-designed spring-assisted burnishing tool, and a pneumatic burnishing tool. A high-quality and precision-engineered rigid burnishing tool was delivered by Taizhou Ke Chi Machinery Company, a reputable manufacturer based in China. This specific burnishing tool, identified by the code JC-SQ8R2030, is designed to deliver exceptional performance and accuracy in various metal finishing applications. The burnishing tool has a 20x20 mm tool shank, providing excellent stability and rigidity during machining.

One notable feature of the burnishing tool is its 30-degree bent tip configuration. This design enables easy access to hard-to-reach areas and facilitates smooth and efficient burnishing operations, particularly in complex workpiece geometries or confined spaces. The bent tip enhances maneuverability and allows for precise control over the burnishing process, resulting in consistent and uniform surface finishes. The burnishing tool incorporates an 8 mm tungsten carbide ball, renowned for its exceptional hardness and wear resistance. Tungsten carbide is preferred for burnishing applications because it can withstand high pressure and maintain its dimensional integrity throughout the machining process. The 8 mm ball size ensures optimal contact with the workpiece surface, enabling effective smoothing and refinement of surface irregularities.

Figure 4 visually represents the burnishing tool, illustrating its key components and dimensions. The depiction showcases the tool shank, the 30-degree bent tip, and the tungsten carbide ball. This visual reference offers a clear understanding of the tool's design and facilitates its proper identification and utilization in manufacturing. By procuring the JC-SQ8R2030 burnishing tool from Taizhou Ke Chi Machinery Company, the aim is to enhance the efficiency and precision of the metal finishing operations. This tool's robust construction, bent tip design, and high-quality tungsten carbide ball enable the achievement of superior surface finishes, ensuring that the final products meet the required specifications and quality standards.

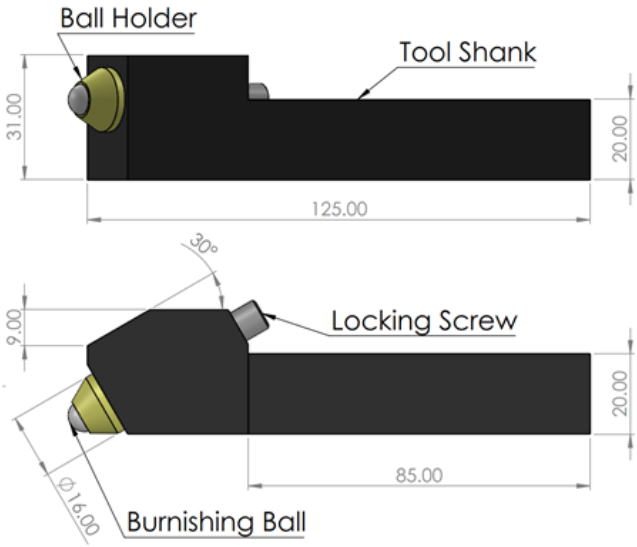

Fig 4. Rigid burnishing tool used in this study, with a tungsten carbide ball, 30° bend tip, and 20×20 mm shank.

For the investigation purpose, a custom-designed spring-assisted burnishing tool was designed and manufactured to achieve the dimensions shown in Figure 5. This tool was purpose-built for the experimental study, incorporating several key design elements and material characteristics to ensure its effectiveness and reliability. The tool shank, an

essential component of the burnishing tool, was fabricated from ASTM T6 high speed tool steel with a width of 20 mm (20×20 mm). The tool steel underwent a series of heat treatments to enhance its mechanical properties, including hardening and tempering. These heat treatments imparted increased hardness, strength, and wear resistance to the tool shank, ensuring its durability and longevity during burnishing. The ball tip of the burnishing tool, responsible for contacting and smoothing the workpiece surface, was constructed using an 8 mm diameter tungsten carbide material.

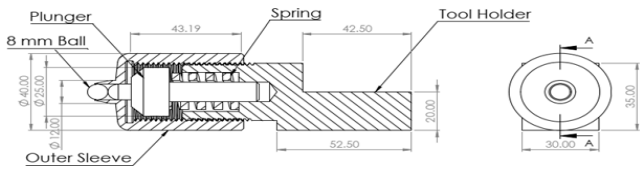

Fig 5. Spring-assisted burnishing tool designed and manufactured with a 20 x 20 mm tool shank.

In this comparative analysis, a third pneumatic burnishing tool, was specifically designed and employed for the study. This tool shares the same tool shank dimensions, tool shank material, and ball tip as the spring-assisted tool. However, it incorporates an air-driven motor for automatic operation, providing distinct advantages regarding convenience and control. Like the spring-assisted tool, the pneumatic burnishing tool utilizes an 8 mm diameter tungsten carbide ball tip. Tungsten carbide, renowned for its hardness and wear resistance, ensures effective material displacement and surface refinement during burnishing. This consistent choice of ball tip material across the tools allows for a fair comparison in terms of performance and outcomes.

However, the pneumatic burnishing tool differentiates itself from the rigid and spring-assisted tools in terms of its operational mechanism. While the rigid tool relies on manual force application and the spring-assisted tool utilizes a spring mechanism, the pneumatic tool utilizes an air-driven motor for automatic operation. This motor-driven approach grants precise control over the burnishing parameters, enabling consistent and reproducible results. The assembly of the pneumatic burnishing tool is visually represented in Figure 6, providing a clear illustration of its components and configuration. The tool incorporates an air compressor that generates a 7-bar pressure applied to the ball tip. This pressurized air creates a constant force exerted during the burnishing process. By employing pneumatic power, the tool ensures a consistent and controlled force application, contributing to the accuracy and reliability of the experimental results.

Using the pneumatic burnishing tool in this comparative analysis allows for a comprehensive evaluation of the burnishing technique, considering different operational mechanisms and their impact on the outcomes. The automatic operation facilitated by the pneumatic motor enhances efficiency and repeatability, while the constant force delivery enables precise control over the burnishing process. Including this tool expands the scope of the investigation, contributing to a more comprehensive understanding of the burnishing technique and its potential applications.

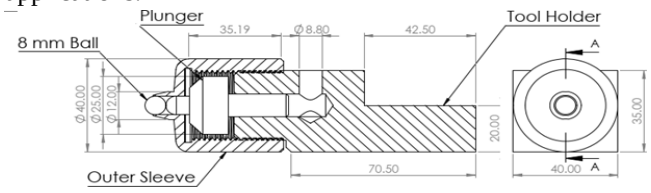

Fig 6. Pneumatic burnishing tool assembly.

2.3 Testing Procedures and Measurements

The research employed the Taguchi experimental test design approach to systematically investigate the effects of various factors on the burnishing process. A total of 16 experiments were conducted per tool using the Taguchi method, ensuring a robust and efficient experimental design. The experimental factors were selected based on three quantitative variables: burnishing speed (N), feed rate (S), and tool depth of ball penetration (h), each chosen at four different levels. The specific levels and corresponding combinations were organized using the Taguchi Array, as presented in Table 3.

The arithmetic average roughness (Ra) and the number of peaks per centimeter (Rpc) were considered to evaluate the surface roughness enhancement. As shown in Fig. 7, these parameters were measured using the Mitutoyo surftest SJ-310, a precision instrument specially designed for surface roughness analysis. A cut-off length of 0.8 mm was selected, ensuring the measurements captured the relevant surface features without excessive influence from longer wavelength variations. The workpiece was divided into three circumferential pieces to ensure comprehensive data collection to identify the optimal measurement locations. Three readings were taken at each designated location, and the arithmetic average of these readings was calculated.

Fig 7. Surface roughness measurements for the burnished workpiece using sj-310 Mitutoyo surftest.

TABLE 3. Study parameters selected for burnishing process.

parameter	Burnishing Speed, N (RPM)	Burnishing Feed, S (mm/rev)	Depth of penetration, h (mm)
1	300	0.09	0.20
2	400	0.10	0.25
3	500	0.11	0.30
4	600	0.12	0.35

A HEXAGON 257 coordinate measuring machine (CMM) was employed to assess the out-of-roundness (O) of the specimens. Utilizing a high-precision measuring instrument ensured reliable and precise measurements of the specimens' dimensional characteristics. The HEXAGON 257 CMM machine provided a sensitivity of 0.1 µm, enabling the detection of minute variations in the specimen's geometry. During the testing process, a total of 100 points were measured around the circumference of each specimen. This comprehensive sampling approach allowed for a thorough evaluation of the out-of-roundness, capturing any deviations from a perfect circular profile. The measurements were taken at equidistant intervals to ensure an even distribution of data points around the specimen's perimeter. Figure 7 presents the obtained measurements for roundness or outwardness. The graphical representation showcases the variations in the specimens' geometry, highlighting any irregularities or deviations from a perfectly round shape. The measurements captured by the HEXAGON 257 CMM machine provide valuable insights into the out-of-roundness characteristics of the specimens, aiding in the quantitative analysis and comparison of different experimental conditions. The experiments carried out as well as the experimental results for this investigation are listed in table 4.

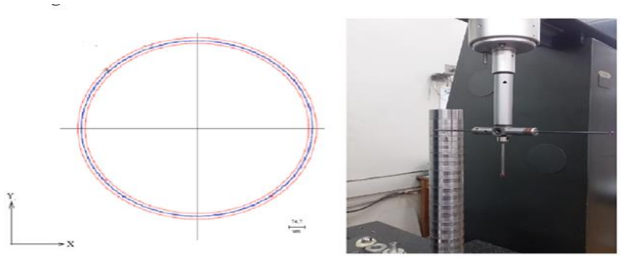

Fig 8. Out of roundness measurements of the workpiece using CMM machine.

3. RESULTS AND DISCUSSIONS

3.1 Mathematical Modelling and Regression Analysis

The relationship between the surface response after burnishing process, encompassing surface roughness factors and out-of-roundness, and the burnishing parameters (burnishing speed (N), burnishing feed rate (S), and tool depth of penetration (h)) for the rigid, spring, and pneumatic tools were mathematically modeled using regression analysis. Table 5 illustrates the regression analysis results, where second-order polynomial response surface parameters were utilized to assess and analyze the experimental data, considering the process factors and their interactions. Applying the student's t- test allowed for evaluating the statistical significance of the identified parameters.

TABLE 4. Taguchi array for L16 design of experiments and study outcomes for different burnishing tools.

No.	N (RPM)	S (mm/rev.)	h (mm)	Rigid Tool			Spring-Assisted Tool			Pneumatic Tool		
				Ra (µm)	Rpc (1/cm)	O (µm)	Ra (µm)	Rpc (1/cm)	O (µm)	Ra (µm)	Rpc (1/cm)	O (µm)
1	300	0.09	0.20	0.22	35.5	11	0.47	66.2	14.9	0.95	123.5	14
2	300	0.10	0.25	0.19	30	8.6	0.46	65.1	15.8	0.83	110.4	15.9
3	300	0.11	0.30	0.18	29.9	8.6	0.43	61.8	16.6	0.84	111.5	16
4	300	0.12	0.35	0.16	26.8	8.4	0.37	55.3	17.2	0.9	118.1	18.8
5	400	0.09	0.25	0.18	29.6	8.9	0.4	58.6	12.9	0.84	111	16.7
6	400	0.10	0.20	0.19	31	10.4	0.43	61.9	11.3	0.78	105	15.6
7	400	0.11	0.35	0.14	25.3	6.3	0.37	55	15.5	0.89	116.9	17.8
8	400	0.12	0.30	0.16	26.2	6.9	0.39	57.5	15.2	0.92	120.2	19.3
9	500	0.09	0.30	0.13	24	7.7	0.41	59.7	16	0.83	110.1	19.4
10	500	0.10	0.35	0.12	23.1	7.3	0.38	56.4	16.5	0.84	111.2	18.9
11	500	0.11	0.20	0.2	31.7	8.9	0.51	70.6	15.6	0.87	114.8	17.7
12	500	0.12	0.25	0.14	26.3	8	0.45	64.1	15.8	0.93	121.3	19.6
13	600	0.09	0.35	0.11	22.1	5.9	0.36	54.2	18.2	0.81	108.2	18.3
14	600	0.10	0.30	0.17	28.5	7.2	0.42	60.8	16.2	0.92	119.8	17.8
15	600	0.11	0.25	0.18	30	7.4	0.5	69.5	15.6	0.82	109.5	18.4
16	600	0.12	0.20	0.19	31.5	9.7	0.51	70.3	14	0.78	105.3	19.5

TABLE 5. Mathematical models for different burnishing responses predicted by RSM method for different burnishing tools.

Tool		Mathematical Models
Rigid Tool	R_a (µm)	0.318 - 0.000569 N + 5.64 S - 1.807 h + 0.000001 N*N - 50.0 S*S - 0.000864 N*h + 16.82 S*h
	Rpc/cm	60.9 - 0.0774 N + 436 S - 220.5 h + 0.000107 N*N - 4687 S*S - 0.0711 N*h + 1907 S*h
	O (µm)	35.2 - 272 S - 56.7 h + 0.000012 N*N + 1125 S*S + 115.0 h*h - 0.0577 N*h
Spring Tool	R_a (µm)	-0.000975 N + 12.99 S + 0.000001 N*N - 57.68 S*S - 1.349 h*h
	Rpc/cm	-0.1029 N + 1692 S + 0.000125 N*N - 7611 S*S - 147.5 h*h
	O (µm)	-0.0564 N + 213.3 S + 96.9 h + 0.000061 N*N - 739 S*h
Pneumatic Tool	R_a (µm)	4.22 - 0.001420 N - 37.5 S - 9.61 h + 106 S*S + 0.00580 N*h + 68.0 S*h
	Rpc/cm	477 - 0.1567 N - 4057 S - 1040 h + 11625 S*S + 0.637 N*h + 7305 S*h
	O (µm)	42.1 + 0.0616 N - 943 S + 40.4 h - 0.000039 N*N + 4687 S*S - 0.0643 N*h

3.2 Effect of Burnishing Parameters on Average Surface Roughness Number (Ra)

3.2.1 Burnishing Speed

Figure 9 (a) illustrates the correlation between the burnishing speed and the surface roughness arithmetic average (Ra) of the workpiece burnished using the rigid tool. The graph reveals important insights into the effect of burnishing speed variation on surface roughness. Initially, as the burnishing speed increases, the surface roughness experiences a decrease, reaching a minimum value of 0.13 µm at a speed of 450 RPM. This reduction in surface roughness can be attributed to the enhanced material displacement and refinement resulting from the higher burnishing speed. However, exceeding the optimal speed threshold may lead to increased surface roughness due to the occurrence of chatter, an undesirable vibration-induced phenomenon [18,19].

Figure 10 (a) illustrates the relationship between the burnishing speed and the surface roughness arithmetic average (Ra) of the workpiece subjected to burnishing using the spring-assisted tool. The graph provides valuable insights into the impact of burnishing speed, feed rate, and penetration depth on surface roughness. The results demonstrate that an increase in burnishing speed leads to a reduction in surface roughness. However, a minimum value of 0.3 µm is observed at a speed of 500 RPM, beyond which further increases in burnishing speed can increase surface roughness. This phenomenon can be attributed to the potential occurrence of chatter, particularly when using the spring setup. Chatter introduces vibrations that compromise the surface finish, leading to an increase in roughness [6,20].

Lastly, Figure 11 (a) depicts the relationship between the burnishing speed and the surface roughness arithmetic average (Ra) of the workpiece subjected to burnishing using the pneumatic tool. The graph shows that an increase in burnishing speed leads to a decrease in surface roughness until it reaches a minimum value of 0.8 µm at a maximum speed of 600 RPM according to the study interval.

3.2.2 Burnishing Feed Rate

Figure 9 (b) depicts the relationship between the feed rate and surface roughness average while using the rigid tool. However, previous studies showed that the surface roughness was decreased as the feed rate increased until it reaches a certain value then it begins to be increased again [18,19]. This study showed a special trend. Notably, when the penetration depth is high, and the feed rate is low, the surface finish of the workpiece improves. This combination decreases surface roughness as the greater penetration depth facilitates more significant plastic deformation, resulting in a smoother surface. Conversely, increasing the feed rate while maintaining the same penetration depth deteriorates the surface quality. This observation highlights the importance of carefully balancing the feed rate and depth of penetration to achieve optimal surface roughness outcomes. It is observed that a minimum value of 0.13 µm is found at a combination of 0.09 mm/rev. feed rate and 0.35 mm depth of penetration.

Figure 10 (b) shows the relationship between surface roughness average and feed rate value subjected to the spring tool. However, previous studies showed that the surface roughness was decreased as the feed rate increased until it reaches a certain value then it begins to be increased again [6-20]. Furthermore, in this study increasing the feed rate is correlated with an increase in surface roughness [21]. This relationship is attributed to the decrease in contact area between the burnishing ball and the workpiece as the feed rate increases. A reduced contact area limits the material flow and deformation, resulting in a less refined surface and higher roughness values. As the results of the study clarifies, a minimum value of 0.3 µm is found at a feed rate of 0.09 mm/rev.

Figure 11 (b) shows the relationship between surface roughness and feed rate when the pneumatic tool is used. At 0.2 mm penetration value, the surface roughness is

enhanced as the feed rate increases until it reaches an optimum value of 0.8 µm at feed rate of 0.11 mm/rev., then it is slightly increase as the feed rate begins to increase again. Combining low penetration depth with a high feed rate decreases surface finish while increasing the feed rate at a high penetration value leads to surface deterioration.

3.2.3 Depth of Penetration

Figure 9 (b) indicates the relationship between the average surface roughness and depth of penetration when the rigid tool is used. The results indicate that increasing the penetration depth has a decreasing effect on surface roughness until it reaches a minimum value of 0.13 µm at a depth of penetration of 0.35 mm. This behavior can be explained by higher penetration depths resulting in more pronounced plastic deformation, leading to smoother surfaces. The increased plastic deformation enhances the material flow and rearrangement, improving surface finish. Otherwise, previous research observed that the surface roughness decreased with increasing the depth of penetration until a certain value then further increasing in penetration leads to increasing in surface roughness [18,19].

Figure 10 (b) depicts the relationship between the average surface roughness and depth of penetration when using spring tool. The increasing penetration depth is found to have a decreasing effect on surface roughness to a minimum value of 0.3 µm at depth of penetration of 0.35 mm according to the study interval. This behavior can be explained by the increase in plastic deformation accompanying higher penetration depths. The enhanced plastic deformation promotes material flow and rearrangement, leading to smoother surfaces and lower roughness values. Otherwise, previous research observed that the surface roughness decreased with increasing the depth of penetration until a certain value then further increasing in penetration leads to increasing in surface roughness [6,20].

Figure 11 (b) depicts the relationship between the average surface roughness and depth of penetration according to using of pneumatic tool in burnishing process. A surface roughness minimum value of 0.8 µm is observed when the depth of penetration adjusted to be 0.2 mm. Further increasing in penetration depth contributes to an increase in surface roughness, which can be attributed to the faster air pressure loss experienced at higher penetration levels. understanding of the influence of burnishing parameters on surface roughness.

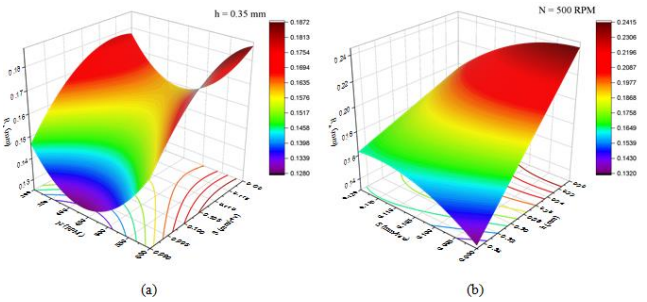

Fig 9. Effect of burnishing parameters on the average surface roughness (Ra) for steel 50 bars burnished by rigid tool.

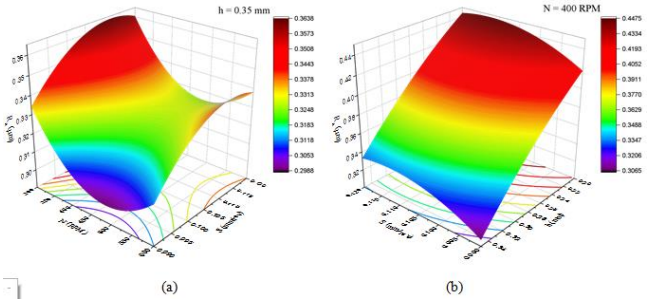

Fig 10. Effect of burnishing parameters on the average surface roughness (Ra) for steel 50 bars burnished by spring tool.

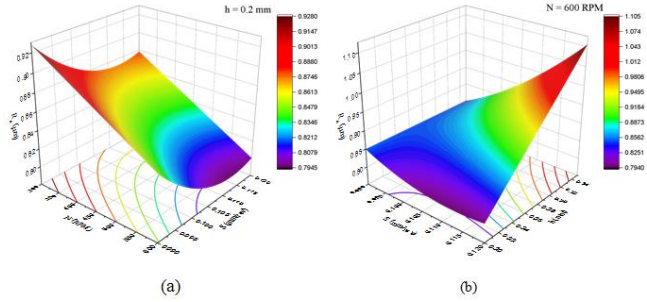

Fig 11. Effect of burnishing parameters on the average surface roughness (R_a) for steel 50 bars burnished by pneumatic tool.

3.3 Effect of Burnishing Parameters on Number of Peaks Per Centimeter (Rpc)

3.3.1 Burnishing Speed

Figure 12 (a) depicts the relationship between the burnishing speed and the number of peaks per centimeter (Rpc) of the workpiece burnished using the rigid tool. The graph reveals crucial insights into the effect of burnishing speed on surface peaks. Initially, as the burnishing speed increases, the surface peaks experience a decline, reaching a minimum value of 20.6 cm-1 at a speed of 500 RPM. This reduction in surface peaks can be attributed to the enhanced material flow and refinement resulting from the higher burnishing speed. However, surpassing the optimal speed threshold may lead to increased surface peaks due to the potential occurrence of chatter, which introduces undesirable vibrations and irregularities to the workpiece surface [18,19].

The findings contribute to Fig. 13 (a) presents the relationship between the burnishing speed and the number

of peaks per centimeter (Rpc) of the workpiece subjected to burnishing using the spring-assisted tool. The graph reveals important insights into the influence of burnishing speed, feed rate, and penetration depth on surface roughness characteristics. The results demonstrate that increased burnishing speed leads to a decrease in surface roughness. However, a minimum value of 51.4 cm-1 is observed at a speed of 425 RPM, beyond which further increases in burnishing speed can increase surface integrities. This behavior is attributed to the potential occurrence of chatter, particularly when using the spring setup. Chatter introduces vibrations that compromise the surface finish, leading to an increase in surface roughness [6,20].

Figure 14 (a) shows the relation between the burnishing speed and the No. Of the workpiece's peaks per centimeter (Rpc) burnished by the pneumatic tool. It is shown that, the surface peaks begin to decrease with the burnishing speed increasing until it reaches a minimum value of 106.5 cm-1 at a maximum speed of 600 RPM according to the study interval.

3.3.2 Burnishing Feed Rate

Figure 12 (b) shows the relationship between the feed rate and surface peaks count while using the rigid tool. However, previous studies showed that the surface roughness was decreased as the feed rate increased until it reaches a certain value then it begins to be increased again [18,19]. This study showed a special trend. Notably, when the penetration depth is high, and the feed rate is low, the surface finish of the workpiece improves. This combination decreases surface roughness as the greater penetration depth facilitates more significant plastic deformation, resulting in a smoother surface. Conversely, increasing the feed rate while maintaining the same penetration depth deteriorates the surface quality. This observation highlights the importance of carefully balancing the feed rate and depth of penetration to achieve optimal surface roughness outcomes. It is observed that minimum peaks count of 20.65 cm-1 is found at a combination of 0.09 mm/rev. feed rate and 0.35 mm depth of penetration.

Figure 13 (b) shows the relationship between surface roughness peaks and feed rate value subjected to the spring tool. However, previous studies showed that the surface roughness was decreased as the feed rate increased until it reaches a certain value then it begins to be increased again [6-20]. Furthermore, in this study increasing the feed rate is correlated with an increase in surface peaks [21]. This relationship is attributed to the decrease in contact area between the burnishing ball and the workpiece as the feed rate increases. A reduced contact area limits the material flow and deformation, resulting in a less refined surface and higher roughness values. As the results of the study clarifies, a minimum value of 51.4 cm-1 is found at a feed rate of 0.09 mm/rev.

Figure 14 (b) shows the relationship between surface integrities and feed rate when the pneumatic tool is used. At 0.2 mm penetration value, the surface roughness is enhanced as the feed rate increases until it reaches an optimum value of 106.5 cm-1 at feed rate of 0.11 mm/rev., then it is slightly increase as the feed rate begins to increase again. Combining low penetration depth with a high feed rate decreases surface finish while increasing the feed rate at a high penetration value leads to surface deterioration.

3.3.3 Depth of Penetration

Figure 12 (b) indicates the relationship between the surface peaks count and depth of penetration when the rigid tool is used. The results indicate that increasing the penetration depth has a decreasing effect on surface roughness until it reaches a minimum value of 20.62 cm-1 at a depth of penetration of 0.35 mm. This behavior can be explained by higher penetration depths resulting in more pronounced plastic deformation, leading to smoother surfaces. The increased plastic deformation enhances the material flow and rearrangement, improving surface finish. Otherwise, previous research observed that the surface roughness decreased with increasing the depth of penetration until a certain value then further increasing in penetration leads to increasing in surface roughness [18,19].

Figure 13 (b) depicts the relationship between the number of peaks and depth of penetration when using spring tool. The increasing penetration depth is found to have a decreasing effect on surface roughness to a minimum value of 51.4 cm-1 at depth of penetration of 0.35 mm according to the study interval. This behavior can be explained by the increase in plastic deformation accompanying higher penetration depths. The enhanced plastic deformation promotes material flow and rearrangement, leading to smoother surfaces and lower roughness values. Otherwise, previous research observed that the surface roughness decreased with increasing the depth of penetration until a certain value then further increasing in penetration leads to increasing in surface roughness [6,20].

Figure 14 (b) depicts the relationship between the peaks count and depth of penetration according to using of pneumatic tool in burnishing process. A surface roughness minimum value of 106.5 cm-1 is observed when the depth of penetration adjusted to be 0.2 mm. Further increasing in penetration depth contributes to an increase in surface roughness, which can be attributed to the faster air pressure loss experienced at higher penetration levels.

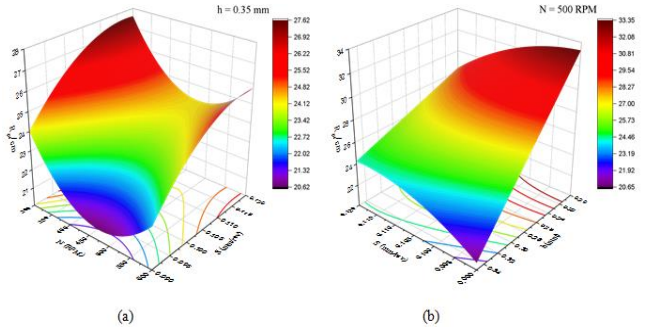

Fig 12. Effect of burnishing parameters on the No. of peaks per centimeter (R_{pc}) for steel 50 bars burnished by rigid tool.

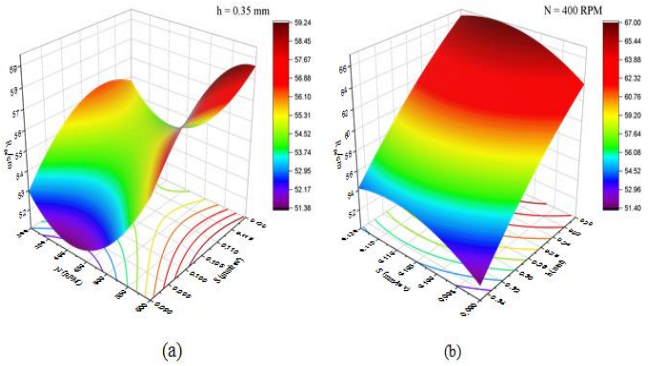

Fig 13. Effect of burnishing parameters on the No. of peaks per centimeter (R_{pc}) for steel 50 bars burnished by spring tool.

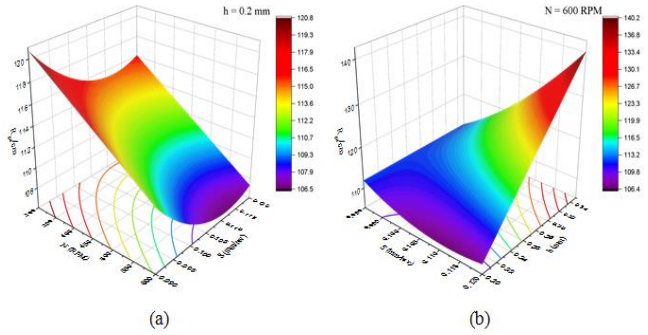

Fig 14. Effect of burnishing parameters on the No. of peaks per centimeter (R_{pc}) for steel 50 bars burnished by pneumatic tool.

3.4 Effect of Burnishing Parameters on Out-of-Roundness (O)

3.4.1 Burnishing Speed

Figure 15(a) presents the relationship between the burnishing speed and the out-of-roundness (O) of the workpiece burnished using the rigid tool. As the burnishing speed increases, the surface out-of-roundness decreases, reaching the minimum value of 5.2 µm at a maximum speed of 600 RPM according to the study interval. This trend can be partially attributed to the fact that the deforming action of the burnishing ball is less pronounced at low speeds and becomes more significant as the speed increases. However, according to previous studies a higher burnishing speeds lead to a significant increase in the roundness error [18,19].

Moving on to Figure 16 (a), it demonstrates the relationship between the burnishing speed and the out-of-roundness (O) of the workpiece subjected to burnishing using the spring-assisted tool. As the burnishing speed increases, the surface out-of-roundness decreases, reaching a minimum value of 12.23 µm at 475 RPM. This reduction is influenced by the possibility of chatter occurrence when using the spring setup, which affects the behavior of the burnishing ball. The vibrations induced by chatter contribute to a more uniform and rounder surface profile.

Figure 17 (a) shows the relation between the burnishing speed and the out-of- roundness (O) of the workpiece burnished by the pneumatic tool. The out-of-roundness minimum value of 13.86 µm is observed at a burnishing speed of 300 RPM according to the study interval. Otherwise, as the burnishing speed increases, the surface out-of-roundness increases.

3.4.2 Burnishing Feed Rate

Figure 15 (b) indicates the effect of burnishing feed rate and roundness error when the rigid tool is used. The out-of- roundness of the burnished surface decreases with increasing feed rate until reach a minimum value of 5.2 µm at a feed rate of 0.12 mm/rev. according to the study interval. This phenomenon may be attributed to the changing contact area between the burnishing ball and the workpiece and the tool's bend angle. The altered contact conditions influence the material flow and deformation, reducing surface irregularities and out- of-roundness. However, previous studies showed that the out-of-roundness was decreased as the feed rate increased until it reaches a certain value then it begins to be increased again [18,19].

Figure 16 (b) indicates the effect of burnishing feed rate and roundness error when the spring tool is used. The combination of low penetration depth and low feed rate leads to a decrease in the out-of-roundness of the workpiece to a value of 12.5 µm at 0.09 mm/rev. feed, while increasing the feed rate at the same penetration value results in surface deterioration. At higher penetration depth, increasing of feed rate value causes a slight enhancement in roundness error, but not to the optimum value.

Figure 17 (b) shows the relation between the burnishing feed rate and the out-of- roundness (O) of the workpiece burnished by the pneumatic tool. The out-of-roundness of the burnished surface decreases with increasing the feed rate until it reaches its minimum value of 13.86 µm at 0.10 mm/rev, then it increases with the feed rate increasing.

This may be due to the contact area change between the ball and the workpiece.

3.4.3 Burnishing depth of Penetration

Figure 15 (b) presents the relationship between the depth of penetration and the out-of-roundness (O) of the workpiece burnished using the rigid tool. As the penetration depth increases, the surface's out- of-roundness experiences a marginal reduction until it reaches a minimum value of 5.2 µm at depth of penetration value 0.35 mm. This can be attributed to the increased ball pressure and greater plastic deformation, which contribute to a more uniform and rounder surface profile. According to previous studies, a further increase in depth of penetration led to out-of-roundness increasing [18,19].

Figure 16 (b) indicates the effect of depth of penetration and roundness error when the spring tool is used. Within the investigated range, a minimum out-of-roundness value of 12.5 µm is obtained at a penetration depth value of 0.2 mm. Otherwise, an increase in penetration depth causes an increase in the out-of-roundness. This increase can be attributed to the spring effect exerted on the burnishing ball, which affects its behavior and introduces subtle irregularities to the workpiece surface.

Figure 17 (b) shows the relation between the burnishing depth of penetration and the out-of- roundness (O) of the workpiece burnished by the pneumatic tool. Within the investigated range, a minimum out-of-roundness value of 13.86 µm is obtained at a penetration depth value of 0.2 mm. Otherwise, an increase in penetration depth causes an increase in the out-of-roundness. The increase in out-of-roundness can be attributed to the decrease of ball pressure on the workpiece due to the high air pressure loss as the penetration value increases.

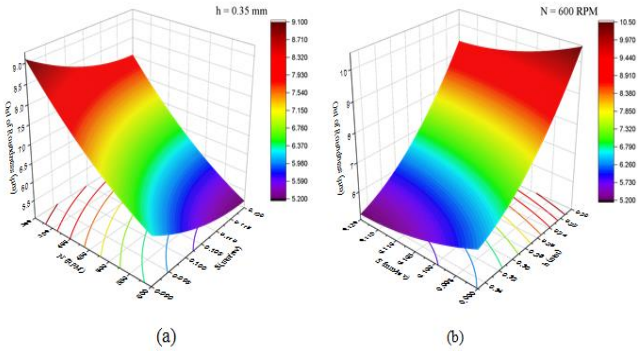

Fig 15. Effect of burnishing parameters on the out-of-roundness (O) for steel 50 bars burnished by rigid tool.

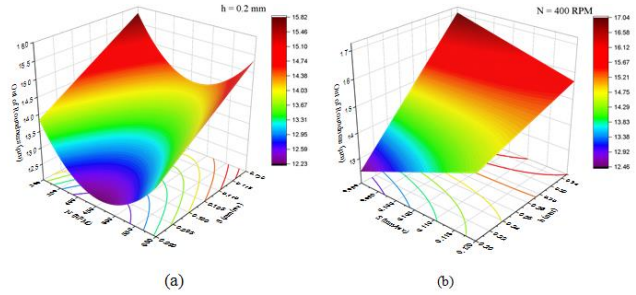

Fig 16. Effect of burnishing parameters on the out-of-roundness (O) for steel 50 bars burnished by spring tool.

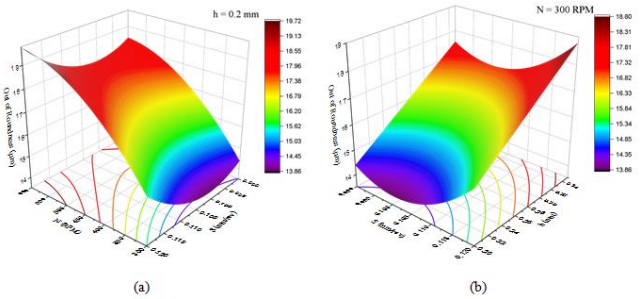

Fig 17. Effect of burnishing parameters on the out-of-roundness (O) for steel 50 bars burnished by pneumatic tool.

4. CONCLUSIONS

This research has undertaken a comprehensive investigation into the influence of tool type on surface roughness and out-of-roundness in the metal burnishing process. Implementing three specifically designed tools and applying a Taguchi L16 matrix, a series of experiments were conducted to evaluate the effects of burnishing parameters. The outcomes of this study have evidenced that the relationship between burnishing parameters and surface roughness, as well as out-of-roundness, is contingent upon both the tool type and the force exerted on the burnishing ball. Notably, optimal parameter combinations were determined for each tool type as follows:

- The rigid tool exhibited a minimum surface roughness value of 0.13 µm with a rotational speed of 450 RPM, a feed rate of 0.09 mm/rev, and a penetration depth of 0.35 mm. While it exhibited a minimum out-of-roundness value of 5.2 µm with a rotational speed of 600 RPM, a feed rate of 0.12 mm/rev, and a penetration depth of 0.35 mm.
- The spring tool achieved a minimum out-of-roundness value of 12.23 µm at a rotational speed of 475 RPM, a feed rate of 0.09 mm/rev, and a penetration depth of 0.20 mm. While it achieved a minimum surface roughness value of 0.3 µm at a rotational speed of 500 RPM, a feed rate of 0.09 mm/rev, and a penetration depth of 0.35 mm.

- The pneumatic tool yielded a minimum surface roughness value of 0.8 µm at a rotational speed of 600 RPM, a feed rate of 0.11 mm/rev, and a penetration depth of 0.20 mm. While it yielded a minimum out-of-roundness value of 13.86 µm at a rotational speed of 600 RPM, a feed rate of 0.11 mm/rev, and a penetration depth of 0.20 mm.

These findings provide valuable insights for optimizing the metal burnishing process and attaining the desired surface quality contingent upon the specific tool type and associated parameters.

REFERENCES

[1] K. A. Prasad and M. R. S. John, "Optimization of external roller burnishing process on magnesium silicon carbide metal matrix composite using response surface methodology," J. Brazilian Soc. Mech. Sci. Eng., vol. 43, no. 7, pp. 1–12, 2021.

[2] L. Prabhu, S. Krishnamoorthi, M. A. Akbar, P. Mubashir, and P. Prashob, "Design and fabrication of ball burnishing tool for surface finish," IOP Conf. Ser. Mater. Sci. Eng., vol. 993, no. 1, 2020.

[3] F. Gharbi, S. Sghaier, K. J. Al-Fadhalah, and T. Benameur, "Effect of ball burnishing process on the surface quality and microstructure properties of aisi 1010 steel plates," J. Mater. Eng. Perform., vol. 20, no. 6, pp. 903–910, 2011.

[4] C. Priyadarsini, V. S. N. V. Ramana, K. A. Prabha, and S. Swetha, "A review on ball, roller, low plasticity burnishing process," Mater. Today Proc., vol. 18, pp. 5087–5099, 2019.

[5] G. Rotella, S. Caruso, A. Del Prete, and L. Filice, "Prediction of surface integrity parameters in roller burnishing of ti6al4v," Metals (Basel)., vol. 10, no. 12, pp. 1–17, 2020.

[6] T. A. El-Taweel and M. H. El-Axir, "Analysis and optimization of the ball burnishing process through the Taguchi technique," Int. J. Adv. Manuf. Technol., vol. 41, no. 3–4, pp. 301–310, 2009.

[7] J. N. Rao, A. C. Reddy, P. V. Rama Rao, "The effect of roller burnishing on surface hardness and surface roughness on mild steel specimens," Int. J. Appl. Eng. Res., Vol. 1, PP. 777-785, 2011.

[8] M. M. El-Khabeery, M. H. El-Axir, "Experimental techniques for studying the effects of milling roller-burnishing parameters on surface integrity," Int. J. Mach. Tools Manuf., Vol.41, PP.1705-1719, 2001.

[9] T. T. Nguyen and M. T. Le, "Optimization of the internal roller burnishing process for energy reduction and surface properties," Stroj. Vestnik/Journal Mech. Eng., vol. 67, no. 4, pp. 167–179, 2021.

[10] M. Fattouh, M. H. El-Axir, and S. M. Serage, "Investigations into the burnishing of external cylindrical surfaces of 70 30 Cu-Zn alloy," Wear, vol. 127, no. 2, pp. 123–137, 1988.

[11] V. Kurkute and S. T. Chavan, "Modeling and Optimization of surface roughness and microhardness for roller burnishing process using response surface methodology for Aluminum 63400 alloy," Procedia Manuf., vol. 20, pp. 542–547, 2018.

[12] T. T. Nguyen, L. H. Cao, X. P. Dang, T. A. Nguyen, and Q. H. Trinh, "Multi-objective optimization of the flat burnishing process for energy efficiency and surface characteristics," Mater. Manuf. Process., vol. 34, no. 16, pp. 1888–1901, 2019.

[13] M. R. S. John and B. K. Vinayagam, "Optimization of nonlinear characteristics of ball burnishing process using Sugeno fuzzy neural system," J. Brazilian Soc. Mech. Sci. Eng., vol. 36, no. 1, pp. 101–109, 2014.

[14] M. R. S. John, A. W. Wilson, A. P. Bhardwaj, A. Abraham, and B. K. Vinayagam, "An investigation of ball burnishing process on CNC lathe using finite element analysis," Simul. Model. Pract. Theory, vol. 62, pp. 88–101, 2016.

[15] M. H. El-Axir, O. M. Othman, and A. M. Abodiena, "Improvements in out-of-roundness and microhardness of inner surfaces by internal ball burnishing process," J. Mater. Process. Technol., vol. 196, no. 1–3, pp. 120–128, 2008.

[16] I. A. Daniyan, K. Mpofu, A. O. Adeodu, and T. M. Azeez, "Investigating the Quality and Conformity of Carbon Steel AISI 1035 under Varying Heat Treatment Conditions," Procedia Manuf., vol. 35, pp. 1111–1116, 2019.

[17] ASTM Standards, "Standard Test Methods for Tension Testing of Metallic Materials 1," 2013.

[18] A. A. Ibrahim, "An investigation into ball burnishing process of carbon steel on a lathe," Al-Azhar engineering 10th international conference, pp. 1–12, 2008.

[19] M. H. El-axir and A. A. Ibrahim, "Some surface characteristics due to center rest ball burnishing," J. Mater. Process. Technol., vol. 167, pp. 47–53, 2005.

[20] A. Tharwat, M. Muhammad, E. Kesba, and F. E. Abu-gharbia, "Improving by Ball Burnishing for Internal Turned Surfaces," IJEAIS, vol. 2, no. 8, pp. 39–50, 2018.

[21] B. Tadic, P. M. Todorovic, and O. Luzanin, "Using specially designed high-stiffness burnishing tool to achieve high-quality surface finish," Int. J. Adv. Manuf. Technol., pp. 601–611, 2013.